Molecular Vision 2014; 20:1605-1611 <http://www.molvis.org/molvis/v20/1605>
Received 22 April 2014 | Accepted 9 November 2014 | Published 11 November 2014

Mass spectrometric analyses of phospholipids in the S334ter-3 rat model of retinal degeneration

Caroline Y. Chen, Byron L. Lam, Sanjoy K. Bhattacharya

Bascom Palmer Eye Institute, University of Miami, Miami, FL

Purpose: The purpose of this study was to profile the endogenous phospholipid species in the retinal tissue of the S334ter-3 rat model of retinal degeneration. Retinal tissue was collected from S334ter-3 rats at postnatal day (P) 20, P30, and P60, while control retinal samples were collected from Sprague-Dawley (SD) rats at the same time points for comparison.

Methods: Lipids were extracted using the Bligh and Dyer method, and resuspended in an acetonitrile/isopropanol (1:1) solution. For lipid analyses, a positive ion–mode precursor ion scan (PIS) was used for phosphatidylcholine (PC; product m/z of 184), a negative ion–mode neutral loss scan (NLS) was used for phosphatidylserine (PS; product m/z of 87.1), and a negative ion–mode PIS was used for phosphatidylinositol (PI; product m/z of 241) and phosphatidylethanolamine (PE; product m/z of 196); the analyses were carried out using a TSQ Quantum Access Max mass spectrometer. The samples were directly infused with a Triversa Nanomate using 1.6 kV and 0.4 psi of pressure for the positive ion mode, and 1.3 kV and 0.6 psi of pressure for the negative ion mode, and scanned for 2 min between 200 m/z and 1000 m/z. Ratiometric quantification was performed using quantitative standards for each lipid class.

Results: The comparative profiles of PC, PE, PS, and PI between S334ter-3 and control rats showed that there were several lipid species common to both groups, as well as several that were unique to the S334ter-3 group and vice versa.

Conclusions: It was found that the proportions of PC and PS were higher in the control retina compared to S334ter-3, and that the proportions of PE and PI were higher in the S334ter-3 retina compared to control.

Retinitis pigmentosa (RP) is a term for a group of genetically heterogeneous retinal degenerations characterized by early rod photoreceptor dysfunction, followed by progressive rod and cone photoreceptor dysfunction and death. This results in nyctalopia, progressive contraction of the visual field, and eventual loss of central vision and blindness. RP is among the leading causes of acquired blindness in the developed world, with a prevalence of 1 in 3,000–4,500 people. Currently, there is no established effective treatment to slow down the progression of RP [1].

Despite its genetic heterogeneity, RP leads to similar phenotypic retinal degenerative changes. Alterations in the photoreceptor function and environment caused by the genetic abnormalities found in RP result in progressive retinal degeneration [2,3]. Photoreceptors are metabolically highly active, and 10% of the outer segment of the rod photoreceptor is renewed and shed daily. The surrounding retinal pigment epithelium (RPE) cells phagocytose the large quantities of visual transduction proteins contained in the outer segment discs. This process requires high amounts of cellular trafficking, protein synthesis, mitochondria, and oxygen, as well as mechanisms to counter oxidative stress and prevent apoptosis.

One approach to elucidating the link between the genetic mutation and the apoptotic death of photoreceptors is to examine the lipid profile alteration under retinal degeneration. Phospholipids play a vital role in the cellular structure and physiology of the retina. They form the lipid bilayers that maintain cell boundaries, in addition to serving as an energy reservoir and precursors for downstream signaling molecules [4]. As such, alterations in the cellular environment may be performed by or reflected in the lipid species present during a disease process. For instance, in a study of diabetic retinopathy, a diabetic-specific increase in vitreous lipid autacoids, including arachidonate- and docosahexaenoate-derived metabolites, was found, supporting the role of inflammation in diabetic retinopathy [5].

Previous studies have demonstrated the potential of lipid analysis to illuminate the disease process of RP. Sphingolipid ceramides function as mediators of apoptosis in several neurodegenerative and neuroinflammatory diseases, including RP [6,7]. The retinal rod outer segment (ROS) membranes are rich in phospholipids that contain docosahexaenoic acid (DHA), and the blood levels of DHA and other long chain polyunsaturated fatty acids are significantly lower in patients with RP as compared to corresponding controls [8]. Furthermore, studies into the relationship between DHA

Correspondence to: Department of Ophthalmology, Bascom Palmer Eye Institute, 1638 NW 10th Avenue, Room 706A, University of Miami, Miami, FL, 33136; Phone: (305) 482-4103; FAX: (305) 326-6547; email: Sbhattacharya@med.miami.edu

and phospholipids have indicated that the reduction in DHA in the ROS membranes of animal models of retinal degeneration is due to decreased incorporation into newly synthesized phospholipids [9]. Therefore, investigation of the phospholipid profile during retinal degeneration may provide insight into the molecular events that occur during RP.

Recent advances in mass spectrometry have enabled highly sensitive and accurate quantification and identification of different lipid species. The mechanism behind RP can be investigated in transgenic animal models that are representations of retinal degeneration in humans. One such model is the S334ter rat line, which expresses a rhodopsin mutation found in human patients [10]. In this study, we present the results of profiling for the phospholipid classes of phosphatidylcholine (PC), phosphatidylethanolamine (PE), phosphatidylserine (PS), and phosphatidylinositol (PI), during the progression of retinal degeneration in the S334ter line 3 (S334ter-3) rat model of RP.

METHODS

Tissue preparation and lipid extraction: At postnatal day (P) 20, P30, and P60, Sprague-Dawley (SD) and S334ter-3 rats were euthanized by CO_2 asphyxiation, and the eyes enucleated under an Institutional Animal Care and Use Committee (IACUC)-approved protocol adhering to the tenets of the *Association for Research in Vision and Ophthalmology* (ARVO) statement for use of animals in research. The anterior segments were removed and the neural retinas were separated from the RPE and flash frozen at −80 °C. Three retinal samples were used for each group—control and all ages (P20, P30, and P60) of S334ter-3 rats. Retinal lipids were extracted using a modified Bligh and Dyer method [11]. The isolated retinal tissue was alternatively thawed in a 37 °C water bath and flash frozen at −80 °C for 5 min, for a total of five freeze–thaw cycles. The tissue was then flushed with argon gas, suspended in 400 µl of 1:1 methanol/chloroform (Sigma-Aldrich, St. Louis, MO), and homogenized for 2 min using a hand-held homogenizer (VWR, Radnor, PA). Following the addition of 350 µl of chloroform, the solution was homogenized for an additional 30 s and subsequently centrifuged at 4 °C for 15 min at 10,000 ×g. The upper aqueous phase containing nonlipid polar molecules was retained for further analysis by PHAST gel, while the lower lipid fraction was flushed with argon gas and the chloroform removed using a Speedvac (Eppendorf, Westbury, NY).

Mass spectrometric analysis: Extracted lipids were resuspended in 1:1 acetonitrile/isopropanol (Sigma-Aldrich) and analyzed in infusion mode using a Triversa Nanomate nanospray (Advion, Ithaca, NY) source on a triple quadrupole mass spectrometer (TSQ Quantum Access Max, Thermo Scientific, San Jose, CA) using previously described parameters appropriate for each of the phospholipid classes [12,13]. For lipid analyses, positive ion–mode precursor ion scan (PIS) was used for PC, negative ion–mode neutral loss scan (NLS) was used for PS, and negative ion–mode PIS was used for PI and PE. Samples were infused with a Triversa Nanomate with a flow rate of 10 µl/ min and scanned for a total of 2.00 min. Scans typically ranged from 200 m/z to 1,000 m/z unless specified otherwise. A peak width was set at 0.7 and collision gas pressure was set at 1 mTorr. Sheath gas (nitrogen) was set to 20 arbitrary units. Auxiliary gas (argon) was set to 5 arbitrary units. For analyses of different phospholipid classes, collision energy (CE), spray voltage, and ion mode were set for each phospholipid class based on established parameters [12], which have been used in our previous studies [13,14]. Briefly, for PC, a CE of 35 V and PIS for m/z 184 was applied. Analyses of PS used NLS for 87.1 at a CE of 24. The PE and PI analyses used CE of 50 and 45 and PIS for m/z 196 and 241.1, respectively. The positive ion mode used formic acid generating protonated species. The Nanomate used 1.6 kV and 0.4 psi of pressure and 1.3 kV and 0.6 psi of pressure for the positive and negative ion modes, respectively. Standards used for each of the phospholipid classes were as follows: PC: 1,2-ditridecanoyl-sn-glycero-3-phosphocholine, product m/z of 184; PE: 1,2-dioleoyl-sn-glycero-3-phosphoethanolamine, product m/z of 196; PS: 1,2-dioleoyl-sn-glycero-3-phospho-L-serine, product m/z of 87.1; PI: 1,2-dioleoyl-sn-glycero-3-phospho-(1'-myo-inositol), product m/z of 241. These were all procured from Avanti Polar Lipids (Alabaster, AL). The additional internal standards 1,2-dioleoyl-sn-glycero-3-phosphoethanolamine-N-(7-nitro-2–1,3-benzoxadiazol-4-yl) and 1,2-dioleoyl-sn-glycero-3-phospho-L-serine-N-(7-nitro-2–1,3-benzoxadiazol-4-yl) were also used for PE and PS, respectively.

Bioinformatics analysis: Identification of lipid species obtained from mass spectrometric analysis was performed using a custom phospholipid database created from LipidMaps (Lipidmaps structure database, LMSD; Nature Lipidomics Gateway, La Jolla, CA) in MZmine 2.10 software. In brief, Thermo RAW files were imported into MZmine and filtered using scan-by-scan filtering, with a range of 200–1,000 m/z for PE, PS, and PI, and 400–900 m/z for PC. Noise (less than E2) was removed and chromatograms constructed using a minimum time span of 0.01 and a tolerance of 1.000 m/z. The CSV files were exported and analyzed using MATLAB to calculate the peak area and standard deviation of the lipid species amounts found in the different S334ter-3 and control groups. Each sample was run with and without internal standards. The internal standards were used

in at least three concentrations added in three independent aliquots of sample and analyzed independently. The resulting data were then analyzed using in-house written Excel macros to determine the presence of phospholipids that were unique to different control or experimental subgroups. All data were normalized to the total amount of phospholipid and are shown as phospholipid ratios.

RESULTS

Lipid profiles for four classes of phospholipid (PC, PE, PS, PI) were obtained for both control and S334ter-3 rats at P20, P30, and P60. A representative PC profile of the control retina with and without internal standard was shown (Figure 1). As mentioned above, lipid amounts were normalized to the total amount of phospholipid, as is shown in the phospholipid ratios. For both control and S334ter-3 retinas, the proportions of PC and PS decreased over time, while the proportion of PE was highest at P30. The proportion of PI increased from P30 to P60 for both control and S334ter-3 retinas (Figure 2). Further analysis of the side chain length of different lipid species was performed, demonstrating that the elevated PE at P30 was largely due to lipid species with a side chain length of 30–39 carbons in both the control and S334ter-3 retina. A progressive decrease in the proportion of the longer (40–52 carbons) PS side chains was observed in the control retina (Figure 3). The lipid species identified using the LMSD and MZmine 2.10 were further analyzed using in-house Excel macros to determine whether certain lipid species were common or unique to the control and S334ter-3 samples (Appendix 1). Various comparisons between different control and S334ter-3 groups showed that most of the lipid species identified were common between both the control and S334ter-3 groups, with only a few species that were unique to each group (Figure 4). For all phospholipid classes, there were several species unique to each time point for both the control and S334ter-3 retina, with the exception of PI in the S334ter-3 group at P30 (Appendix 1). Overall, it was found that the proportions of PC and PS were higher in the control retina as compared to the S334ter-3 retina, and that the proportions of PE and PI were higher in the S334ter-3 retina as compared to the control (Figure 5).

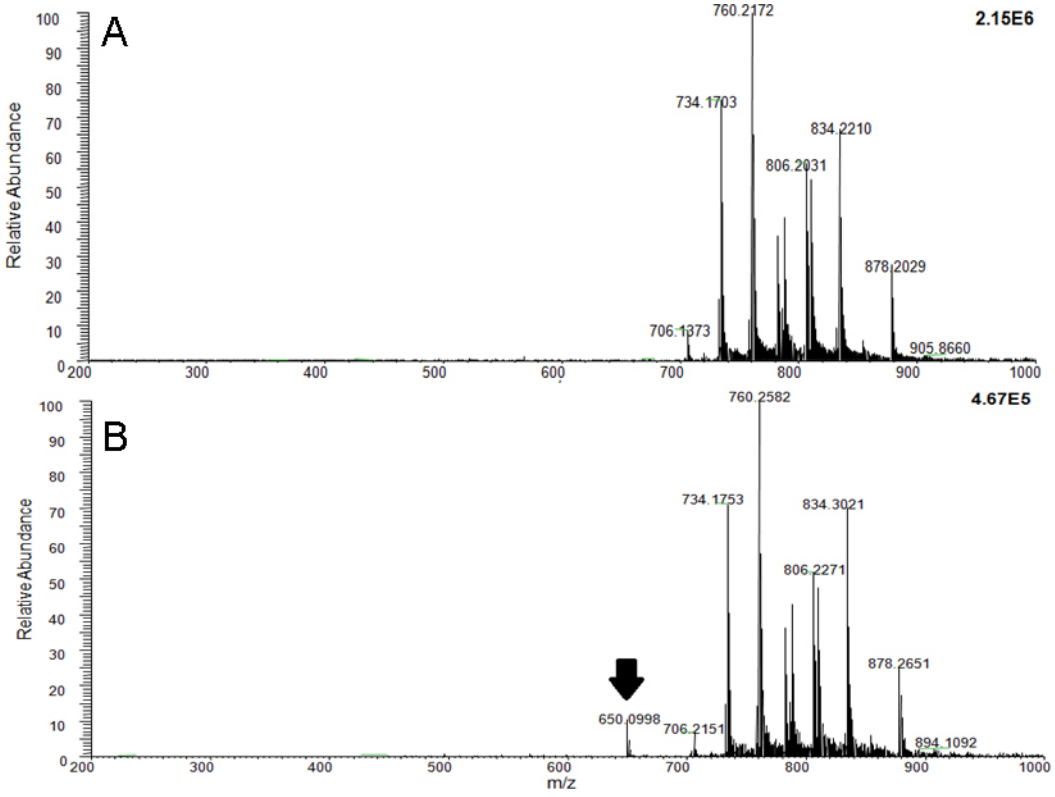

Figure 1. Representative electrospray ionization tandem mass spectrometric analysis of phosphatidylcholine (PC) extracted from control rats in positive ion mode. **A**: Representative precursor ion scan (PIS) scanning for m/z 184, characteristic of the PC class of lipids. **B**: Representative PIS scanning for m/z 184, including an internal standard (m/z ratio of 650) for ratiometric quantification.

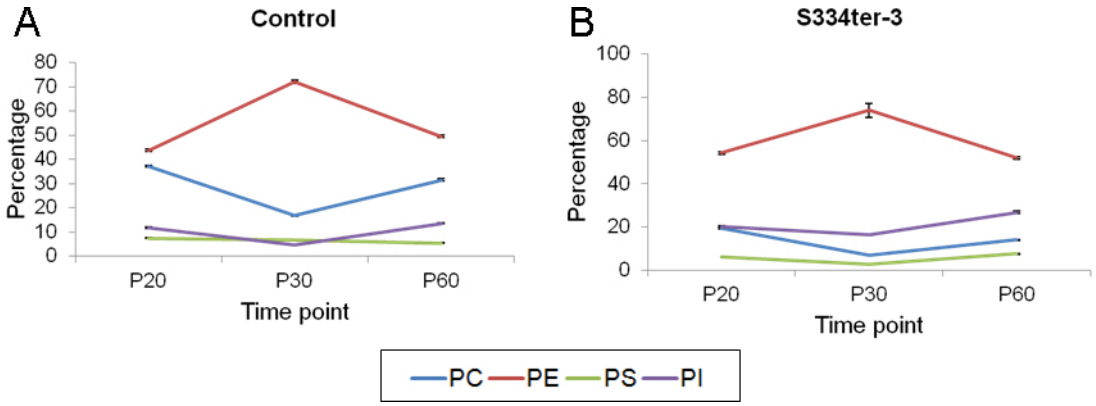

Figure 2. Total phospholipid in control and S334ter-3 rats over time. Proportions of phosphatidylcholine (PC), phosphatidylethanolamine (PE), phosphatidylserine (PS), and phosphatidylinositol (PI) found in control and S334ter-3 rats at postnatal day (P) 20, P30, and P60 (n = 3) are shown as percentages. The mean ± standard deviation results derived from n = 3 samples are shown.

DISCUSSION

In this study, we presented a comprehensive profile of the phospholipid species in the S334ter-3 rat model of RP, which highlighted the differences in membrane composition caused by retinal degeneration; this may ultimately improve our understanding and treatment of the disease. There have been several studies using different neurotrophic factors such as ciliary neurotrophic factor (CNTF), glial-derived neurotrophic factor (GDNF), brain-derived neurotrophic factor (BDNF), and fibroblast growth factors (FGF) such as FGF-5 and FGF-18, in an effort to prevent photoreceptor cell death in different animal models of retinal degeneration [15-17]. Several have had promising results, with the increased expression of neurotrophic factor resulting in decreased photoreceptor cell death, although this sometimes failed to correlate with increased electroretinogram activity. This discrepancy between the structural and functional results warrants further investigation into the mechanism of the protective effect these neurotrophic factors exert, largely through the receptor tyrosine kinase (RTK) pathway. RTKs have been known to associate with lipid rafts, which are composed of a variety of cholesterols, phospholipids, and sphingolipids. The different lipid compositions of these rafts have an impact in determining the location and number of associated RTKs, and how well they function [18].

Our results indicate a progressive decrease in the proportion of PCs over time in the S334ter-3 retina, which could reflect progressive photoreceptor cell death. PCs are

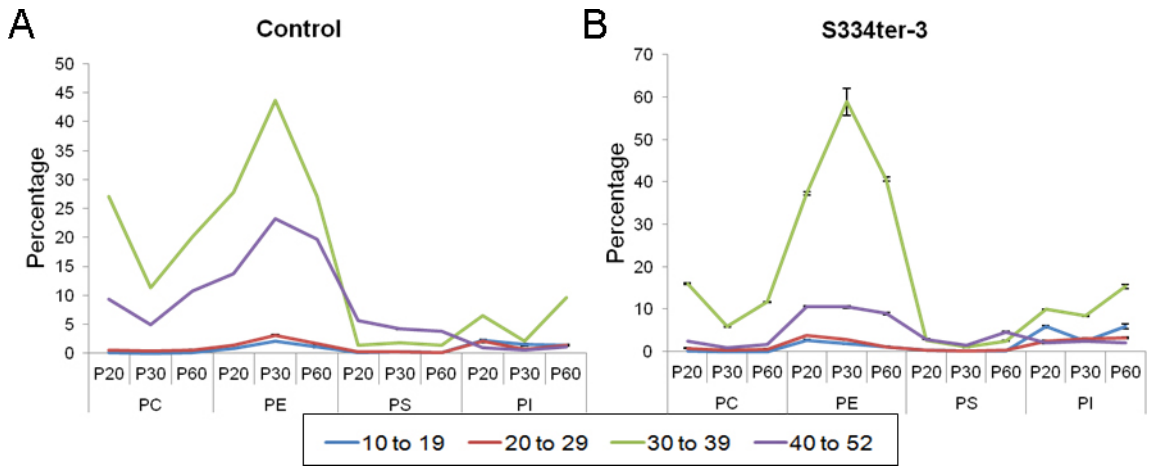

Figure 3. Phospholipid side chain distribution over time. Proportions of phosphatidylcholine (PC), phosphatidylethanolamine (PE), phosphatidylserine (PS), and phosphatidylinositol (PI) species found in control and S334ter-3 rats shown as percentages, distributed according to the number of carbons present in each of the side chains at postnatal day (P) 20, P30, and P60. The mean ± standard deviation results derived from n = 3 samples are shown.

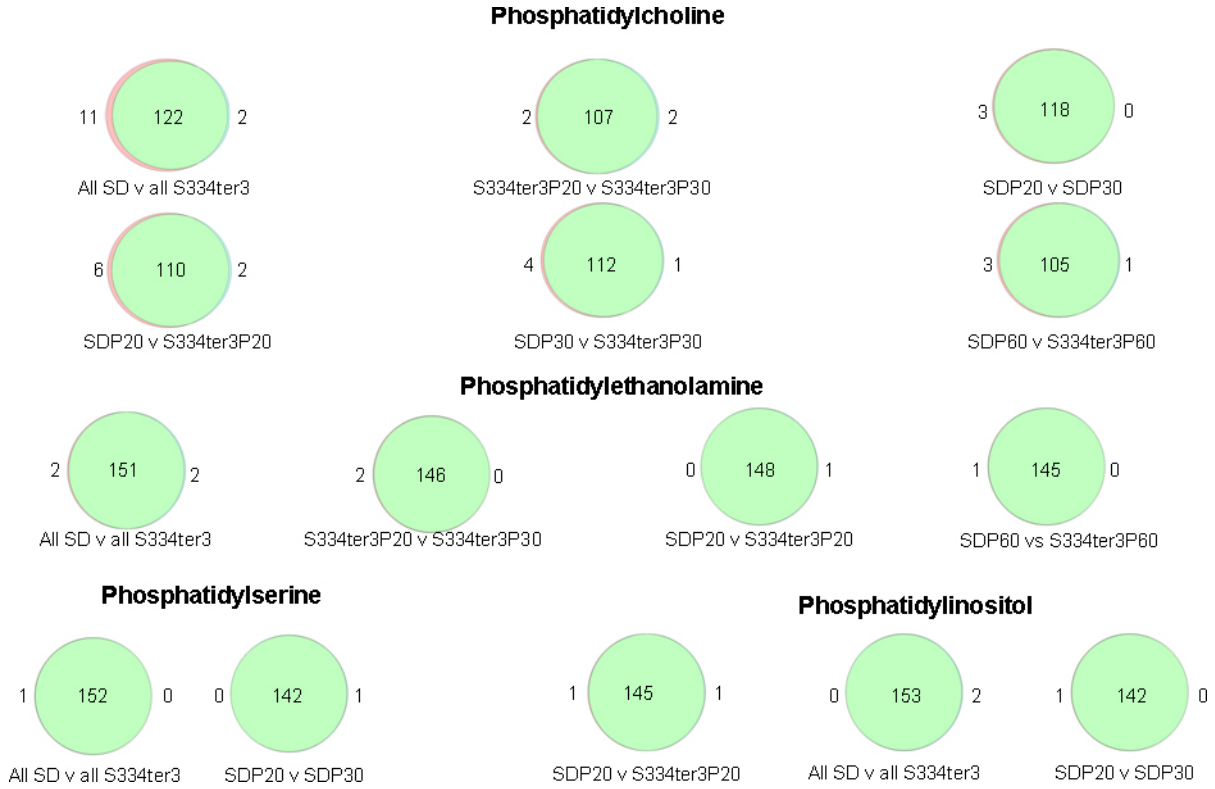

Figure 4. Venn diagrams comparing phosphatidylcholine (PC), phosphatidylethanolamine (PE), phosphatidylserine (PS), and phosphatidylinositol (PI) species in control and S334ter-3 retinas. The numbers represent the PC, PE, PS, and PI species found to be unique or common in control and S334ter-3 rat retinas at postnatal day (P) 20, P30, and P60. The red and green circles represent the first versus second described organism below each circle respectively.

vital to maintain the structural integrity of the lipid bilayer membrane. Although a similar decrease was observed in the control retina, the proportion of PC starting at P20 was greater in the control mice, and decreased to a lesser degree over time. Previous studies on the *rd11* mouse model of retinal dystrophy have also shown the importance of PCs in retinal degeneration. Through linkage analysis, it was found that mutation of the *rd11* locus led to a truncated lysophosphatidylcholine acyltransferase-1 (LPCAT1) protein, which carries out the conversion of palmitoyl-lysophosphatidylcholine to dipalmitoyl-PC (DPPC) [19]. This demonstrates that mutations in a metabolic pathway of PC can have a large role in photoreceptor function and their potential role in retinal degeneration may be of interest. Although the *rd11* mice did in fact have lower levels of DPPC suggesting a link to the retinal degeneration, follow-up screening in patients

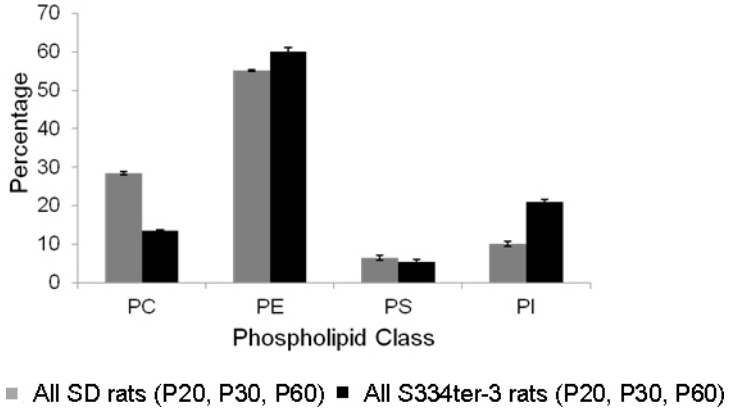

Figure 5. Total phospholipid in control and S334ter-3 rats. Proportions of phosphatidylcholine (PC), phosphatidylethanolamine (PE), phosphatidylserine (PS), and phosphatidylinositol (PI) are shown as percentages. Control and S334ter-3 species are represented by gray and black bars, respectively, as indicated. The mean ± standard deviation results derived from n = 3 samples are shown.

with RP and similar degenerative disorders such as Leber congenital amaurosis did not demonstrate any striking pathogenic mutations in LPCAT1. Our analyses, however, did not identify DPPC species in either the control or experimental animals. This does not appear to be the result of our analytical method, as a synthetic standard was correctly identified by our instrument using these parameters.

Overall, PEs were significantly higher in the S334ter-3 samples, initially increasing from P20 to P30, and then decreasing from P30 to P60. This may be due to mutations in the ABCA4 protein, a member of the family of ATP binding cassette transporters that has been implicated in RP and other retinal degenerative diseases, such as cone–rod dystrophy, Stargardt macular degeneration, and age-related macular degeneration [1,20-22]. Studies have shown that ABCA4 facilitates the clearance of all-trans retinal (ATR) from photoreceptors following photoexcitation, which prevents the potentially toxic build-up of ATR. Specifically, it binds *N*-retinylidene-PE, which is the Schiff's base adduct of retinal and PE, and then pumps it from the lumenal to the cytoplasmic side of the disc membranes. Knockout mice that lack ABCA4 accumulate toxic levels of ATR, PE, and *N*-retinylidene-PE in their retinal tissue, resulting in a buildup of lipofuscin in RPE cells and compromised dark adaptation. If an ABCA4 mutation was present in the S334ter-3 model of RP, this may explain the significantly higher levels of PE at P30 as *N*-retinylidene-PE built up, and the decrease in PE at P60 as that toxic build-up led to cell death.

PSs were found to be slightly lower overall in the S334ter-3 group. This may be explained by the higher overall PE also found in the S334ter-3 group. PS can be converted to PE in the mitochondria via PS decarboxylase 1. The resulting PE produced can then be exported to constitute other membranes within the cell [20-23]. Further study is needed to investigate whether or not those enzymes responsible for the PS to PE conversion are upregulated in RP.

PI increased from P30 to P60 for both control and S334ter-3 retina, but to a greater degree in the S334ter-3 retina. Previous studies on *Drosophila melanogaster* have demonstrated that phospholipase D (Pld)-null flies are more susceptible to retinal degeneration [24]. Pld, an enzyme also found in mammalian retina and ROSs, regenerates the supply of PI available to generate PI 4,5-bisphosphate (PIP2), a key signaling compound. The proposed mechanism is that Pld generates phosphatidic acid from PCs, which can then be converted to PI. Since those flies lacking Pld are prone to retinal degeneration, seemingly due to a lack of PIP2 formation, it is possible that the significantly increased PI in the S334ter-3 rats was due to the decreased hydrolysis of PI to form PIP2, which may contribute to retinal degeneration.

As lipids play a crucial role in the structure, function, and maintenance of homeostasis in the retina, it is of interest to profile the different lipid species present in the retina of nontreatable causes of blindness such as RP. Although the functions of many of the phospholipid species identified in this paper have yet to be determined, their presence or absence may elucidate the molecular changes in signaling present in RP, identify new targets for further investigation, and ultimately improve our understanding and treatment of this disease.

APPENDIX 1.

To access the data, click or select the words "Appendix 1."

ACKNOWLEDGMENTS

This work was partially supported by DOD grant W81XWH-09-1-0674 (Project 4.2) and unrestricted funds from Research to Prevent Blindness and NIH core grant P30EY14801.

REFERENCES

1. Werdich XQ, Place EM, Pierce EA. Systemic diseases associated with retinal dystrophies. Semin Ophthalmol 2014; 29:319-28. [PMID: 25325857].
2. Mitamura Y, Mitamura-Aizawa S, Nagasawa T, Katome T, Eguchi H, Naito T. Diagnostic imaging in patients with retinitis pigmentosa. The journal of medical investigation JMI 2012; 59:1-11. [PMID: 22449988].
3. Green ES, Menz MD, LaVail MM, Flannery JG. Characterization of rhodopsin mis-sorting and constitutive activation in a transgenic rat model of retinitis pigmentosa. Invest Ophthalmol Vis Sci 2000; 41:1546-53. [PMID: 10798675].
4. Ghanem AA, Mady SM, El Awady HE, Arafa LF. Homocysteine and hydroxyproline levels in patients with primary open-angle glaucoma. Curr Eye Res 2012; 37:712-8. [PMID: 22458818].
5. Schwartzman ML, Iserovich P, Gotlinger K, Bellner L, Dunn MW, Sartore M, Grazia Pertile M, Leonardi A, Sathe S, Beaton A, Trieu L, Sack R. Profile of lipid and protein autacoids in diabetic vitreous correlates with the progression of diabetic retinopathy. Diabetes 2010; 59:1780-8. [PMID: 20424229].
6. Strettoi E, Gargini C, Novelli E, Sala G, Piano I, Gasco P, Ghidoni R. Inhibition of ceramide biosynthesis preserves photoreceptor structure and function in a mouse model of retinitis pigmentosa. Proc Natl Acad Sci USA 2010; 107:18706-11. [PMID: 20937879].
7. Rotstein NP, Miranda GE, Abrahan CE, German OL. Regulating survival and development in the retina: key roles for

simple sphingolipids. J Lipid Res 2010; 51:1247-62. [PMID: 20100817].

8. Converse CA, Hammer HM, Packard CJ, Shepherd J. Plasma lipid abnormalities in retinitis pigmentosa and related conditions. Trans Ophthalmol Soc U K 1983; 103:508-12. [PMID: 6591588].

9. Martin RE, Fliesler SJ, Brush RS, Richards MJ, Hopkins SA, Anderson RE. Lipid differences in rod outer segment membranes of rats with P23H and S334ter opsin mutations. Mol Vis 2005; 11:338-46. [PMID: 15928607].

10. Ray A, Sun GJ, Chan L, Grzywacz NM, Weiland J, Lee EJ. Morphological alterations in retinal neurons in the S334ter-line3 transgenic rat. Cell Tissue Res 2010; 339:481-91. [PMID: 20127257].

11. Bligh EG, Dyer WJ. A rapid method of total lipid extraction and purification. Can J Biochem Physiol 1959; 37:911-7. [PMID: 13671378].

12. Bhattacharya SK. Recent advances in shotgun lipidomics and their implication for vision research and ophthalmology. Curr Eye Res 2013; 38:417-27. [PMID: 23330842].

13. Aribindi K, Guerra Y, Lee RK, Bhattacharya SK. Comparative phospholipid profiles of control and glaucomatous human trabecular meshwork. Invest Ophthalmol Vis Sci 2013; 54:3037-44. [PMID: 23557733].

14. Edwards G, Aribindi K, Guerra Y, Lee RK, Bhattacharya SK. Phospholipid Profiles of Control and Glaucomatous Human Aqueous Humor. Biochimie 2014; 101:232-47. [PMID: 24561385].

15. Liang FQ, Aleman TS, Dejneka NS, Dudus L, Fisher KJ, Maguire AM, Jacobson SG, Bennett J. Long-term protection of retinal structure but not function using RAAV.CNTF in animal models of retinitis pigmentosa. Molecular Gene Therapy. 2001; 4:461-72. [PMID: 11708883].

16. Green ES, Rendahl KG, Zhou S, Ladner M, Coyne M, Srivastava R, Manning WC, Flannery JG. Two animal models of retinal degeneration are rescued by recombinant adeno-associated virus-mediated production of FGF-5 and FGF-18. Molecular Gene Therapy. 2001; 3:507-15. [PMID: 11319911].

17. Gregory-Evans K, Chang F, Hodges MD, Gregory-Evans CY. Ex vivo gene therapy using intravitreal injection of GDNF-secreting mouse embryonic stem cells in a rat model of retinal degeneration. Mol Vis 2009; 15:962-73. [PMID: 19461934].

18. Pontier SM, Schweisguth F. Glycosphingolipids in signaling and development: from liposomes to model organisms. Developmental Dynamics American Association of Anatomists. 2012; 241:92-106. [PMID: 22038940].

19. Friedman JS, Chang B, Krauth DS, Lopez I, Waseem NH, Hurd RE, Feathers KL, Branham KE, Shaw M, Thomas GE, Brooks MJ, Liu C, Bakeri HA, Campos MM, Maubaret C, Webster AR, Rodriguez IR, Thompson DA, Bhattacharya SS, Koenekoop RK, Heckenlively JR, Swaroop A. Loss of lysophosphatidylcholine acyltransferase 1 leads to photoreceptor degeneration in rd11 mice. Proc Natl Acad Sci USA 2010; 107:15523-8. [PMID: 20713727].

20. Quazi F, Lenevich S, Molday RS. ABCA4 is an N-retinylidene-phosphatidylethanolamine and phosphatidylethanolamine importer. Nature Communications. 2012; 3:925-[PMID: 22735453].

21. Pollock NL, Callaghan R. The lipid translocase, ABCA4: seeing is believing. FEBS J 2011; 278:3204-14. [PMID: 21554544].

22. Goldberg AF, Molday RS. Subunit composition of the peripherin/rds-rom-1 disk rim complex from rod photoreceptors: hydrodynamic evidence for a tetrameric quaternary structure. Biochemistry 1996; 35:6144-9. [PMID: 8634257].

23. Schuettauf F, Rejdak R, Walski M, Frontczak-Baniewicz M, Voelker M, Blatsios G, Shinoda K, Zagorski Z, Zrenner E, Grieb P. Retinal neurodegeneration in the DBA/2J mouse-a model for ocular hypertension. Acta Neuropathol 2004; 107:352-8. [PMID: 14745571].

24. LaLonde MM, Janssens H, Rosenbaum E, Choi SY, Gergen JP, Colley NJ, Stark WS, Frohman MA. Regulation of phototransduction responsiveness and retinal degeneration by a phospholipase D-generated signaling lipid. J Cell Biol 2005; 169:471-9. [PMID: 15883198].

Articles are provided courtesy of Emory University and the Zhongshan Ophthalmic Center, Sun Yat-sen University, P.R. China. The print version of this article was created on 11 November 2014. This reflects all typographical corrections and errata to the article through that date. Details of any changes may be found in the online version of the article.